Stress-activated neuronal ensemble in the supramammillary nucleus stores anxiety but not memory

Jinming Zhang[1], Kexin Yu[1], Junmin Zhang[1], Yuan Chang[2], Xiao Sun[1], Zhaoqiang Qian[3], Zongpeng Sun[4], Zhiqiang Liu[1], Wei Ren[1,5], Jing Han[1,6,*]

1. Key Laboratory of Modern Teaching Technology, Ministry of Education, Shaanxi Normal University, Xi'an, 710062, China
2. Department of Histology and Embryology, School of Basic Medical Science, Xi'an Medical University, Xi'an, 710021, China
3. Laboratory Animal Center, Shaanxi Normal University, Xi'an, 710119, China
4. School of Psychology, Shaanxi Normal University, Xi'an, 710062, China
5. Faculty of Education, Shaanxi Normal University, Xi'an, 710062, China
6. Lead contact

***Correspondence:** Jing Han: jhan2012@snnu.edu.cn

Abstract

Anxiety is a very common negative emotional status induced by stress. However, its underlying neural mechanism is still largely unknown. Here, we found a hypothalamic section named the supramammillary nucleus (SuM), which is taking control of anxiety. We then characterized a small ensemble of stress-activated neurons and recruited encoding anxiety. These stress-activated neurons specifically respond to stress, and its activation robustly increases the anxiety-like behavior of mice without significantly influencing fear memory. We then found that the ventral subiculum -SuM but not the dorsal subiculum -SuM projection encodes anxiety and would exhibit an anti-anxiety effect by its inhibition. Our findings extend the understanding of the function of the neuronal engram cells and bring new insights into the studies on emotion especially anxiety.

Keywords

Supramammillary nucleus, Subiculum, Anxiety, Engram cells

Introduction

Anxiety is a fundamental negative emotion across almost all species of mammals. Long-lasting and uncontrollable anxiety often leads to several mental disorders, anxiety disorders, and even depression(Nettle & Bateson, 2012). Recent studies have shown that the supramammillary nucleus (SuM), a part of the hypothalamus, regulating sleep(Liang et al., 2023), memory(Chen et al., 2020; Y. Li et al., 2020), novelty exploration(Chen et al., 2020; Kesner et al., 2021), social memory(J. Li et al., 2022; Qin et al., 2022), neurogenesis(Y. D. Li et al., 2022), consciousness(Pedersen et al., 2017), locomotion activity(Farrell et al., 2021), and theta oscillation in the hippocampus(Pan & McNaughton, 2002). Its efferent on the hippocampus has been largely studied and was found to modulate either episodic memory(Chen et al., 2020) or social memory(J. Li et al., 2022; Qin et al., 2022), regarding the different downstream subareas of the hippocampus. Although SuM locates very close to mammillary nucleus, a key subarea in the regulation of emotion indicated by the Papez's circuit, its role in regulating emotion has only been superficially explored without in-depth investigation. Although it has been discussed a few times, contrast still exists across reports and no consistent conclusion has been reached so far(Y. D. Li et al., 2022; López-Ferreras et al., 2019, 2020).

Engram cells have been tagged and studied in many brain areas(Josselyn & Tonegawa, 2020; Tonegawa et al., 2015). These tagged engram cells reacted to specific stimulation and mediated the storage and retrieval of relevant memory, such as conditional stimulus(Guenthner et al., 2013; Liu et al., 2012), pain(H. Sun et al., 2023), food(Azevedo et al., 2019), and even periphery inflammation(Koren et al., 2021). The manipulation of engrams can rescue the pathology of neurodegeneration disease(Ryan et al., 2015) or inflammation(Koren et al., 2021), suggesting its strong potential as a therapeutic target. Naturally, this led us to think about whether there are special engram cells that encode anxiety. In contrast to the abovementioned topics, few studies reported emotion-related engram cells(T. R. Zhang et al., 2019). Recent studies have focused on the role of the hippocampus and its relevant neuronal afferents and efferent(Forro et al., 2022; Jimenez et al., 2018; Yan et al.,

2022). The dorsal part of the hippocampus mainly contributes to cognitive processes, while the ventral hippocampus is often associated with emotion(Fanselow & Dong, 2010; Strange et al., 2014). Even the ventral hippocampus-hypothalamus circuit was reported to modulate anxiety(Jimenez et al., 2018; Yan et al., 2022), and it is still unknown if SuM also works as a part of this modulation system. SuM sends and receives dense neuronal projections, but few studies focus on its afferents, not to mention its modulation of behavior and emotion(Kesner et al., 2023).

At this moment in this study, we first use multiple methods to confirm if SuM will respond to stress events, both acute and chronic stress. And chemogenetically manipulate the activity of SuM and test the anxiety-like behavior in rodents. Then, we utilized the targeted recombination in active populations (TRAP) strategy to label and manipulate the stress-activated neurons in SuM to verify if these cells can be tagged as engram cells. After clearly showing how SuM modulates anxiety, we tended to trace the upstream brain area that may contribute to the supramammillary function. The effect of neuronal projection from vSub to SuM was also tested using fiber photometry of calcium dynamics and chemogenetic manipulation. After gathering these results, we describe an anxiety-specific engram cell ensemble, which has not been reported in SuM previously. In addition, we showed the projection from the ventral part of the Sub but not the dorsal part of it to SuM, governing the chronic stress-induced anxiety-like behaviors.

Results

1. Stress increases the level of neuronal activity in SuM

We verified an acute stress protocol consisting of foot-shocks, then tested mice with EPM and EZM to estimate anxiety in Day 2 and Day 7 (Figure 1. A). Mice who experienced foot-shock showed a decrease in traveling distance and exploration time in open arms on Day 2. While acute stress-induced anxiety cannot be detected on Day 7 (Figure 1. B-D). The c-Fos protein expression and the Ca^{2+} concentration were inspected after acute stress to test if the SuM is activated. The number of the c-Fos^{+} cell was significantly increased by foot-shock (Figure 1. E-G). The somatic Ca^{2+} activity was also increased immediately by foot-shock (Figure 1. H-J). We then tested if chronic stress affects the neuronal activity of SuM. In vivo electrophysiological recording showed that regular-spiking neurons spiked more after CSDS (Figure 1. K-M) while fast-spiking neurons did not (Supplemental Figure 1. A-B). Regarding the local field potential, mice from the naïve and CSDS groups didn’t show any noticeable difference in the power spectrum analysis (Supplemental Figure 1. C-D). These results indicated that acute and chronic stress could strongly activate the supramammillary nucleus.

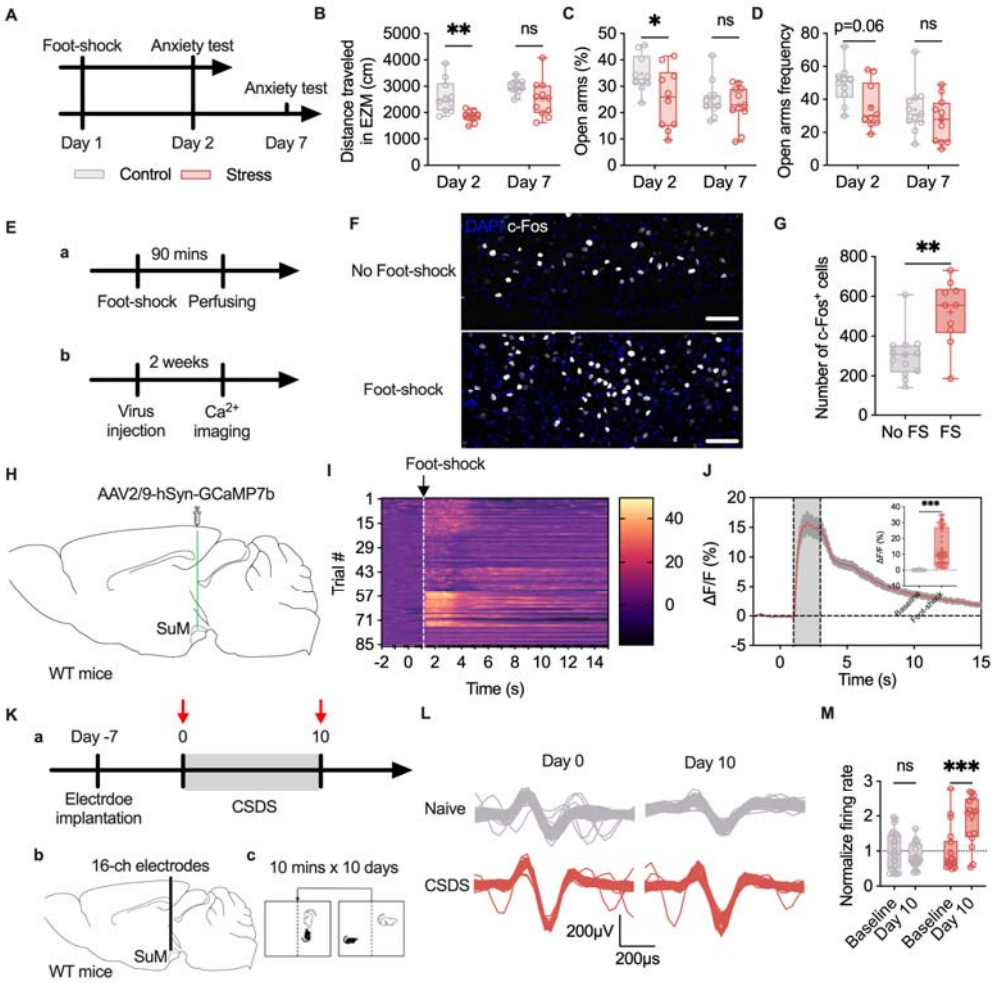

Figure 1. Stress activates the supramammillary nucleus

(A) Workflow of acute stress and anxiety tests.

(B) Statistical comparison of the distance that mice spent in EZM. n = 10-11 per group, two-way ANOVA, Sidak's post-hoc test.

(C) Statistical comparison of the time that mice spent in open arms of EZM. n = 10-11 per group, two-way ANOVA, Sidak's post-hoc test.

(D) Statistical comparison of the frequency that mice enter into open arms of EZM. n = 10-11 per group, two-way ANOVA, Sidak's post-hoc test.

(E) Workflow of c-Fos staining (a) and Ca^{2+} imaging (b).

(F) Representative images of c-Fos staining (DAPI: blue, c-Fos: white, scale bar: 50μm).

(G) Statistical comparison of the number of c-Fos positive cells displayed in panel B. n = 10-13 per group, unpaired t-test.

(H) Virus injection information for Ca^{2+} imaging.

(I) Heatmap of Ca^{2+} fluorescent intensity before and after foot-shocks.

(J) Averaged ΔF/F of Ca^{2+} before and after foot-shocks; and statistical comparison of the peak of Ca^{2+} activity. n = 60 per group, Wilcoxon matched-pairs test.

(K) Workflow of CSDS (a, c) and electrode implantation (b).

(L) Representative spikes acquired by multi-channel recording.

(M) Statistical comparison of the firing rate of RNs between baseline and after CSDS. n = 16-23 per group, two-way ANOVA, Sidak's post-hoc test. Data in C, F and I are presented as Mean ± SEM. "**"p <0.01, "***"p < 0.001. CSDS: Chronic social stress; FS: Foot-shock. Also see **Supplemental Figure 1.**

2. SuM modulates anxiety-like behavior

To further investigate if SuM encodes and mediates the behavior of anxiety in mice, in vivo multi-channel recording and chemogenetic manipulation were conducted. Experiments were performed as the workflow shows (Figure 2. A). When focusing on the transition from the closed arms to the open arms of EPM, regular-spiking neurons (RNs) presented a much lower firing rate (Figure 2. B). In contrast, the firing rate of fast-spiking neurons (FNs) didn't change across the transition (Figure 2. C). On the other hand, when focusing on the transition from the open arms to the closed arms of the EPM, the firing rate of RNs didn't change (Figure 2. D), while FNs showed a much higher firing rate (Figure 2. E). These data suggested that SuM is involved in encoding anxiety-like behavior of mice in EPM. We then tested if manipulating the neuronal activity of SuM would influence the anxiety-like behavior of mice. Mice were introduced into OF and EZM tests at least 2 weeks after virus injection, followed by a reward-seeking test (Figure 2. F-G, Supplemental Figure 2. A). CNO was applied intraperitoneally 30 minutes before the test. Chemogenetic activation of SuM didn't change the performance of mice in OF (Figure 2. C-D, Supplemental Figure 2. B). SuM-activated mice explored the open arms of the EZM less than control mice (Figure 2. E), with no modification on the moving distance (Supplemental Figure 2. C). Moreover, SuM-activated mice ate less than controlled mice (Figure 2. F). SuM-inactivated mice moved less distance than controlled mice (Supplemental Figure 2. D) in OF. Still, no difference was observed when analyzing moving distance in the central area and time spent in the central region (Figure 2. G-H). No significance was observed in EZM and reward-seeking tests (Figure 2. I-J, Supplemental Figure 2. E). These data suggested that there are neuronal ensembles that control the expression of anxiety behavior.

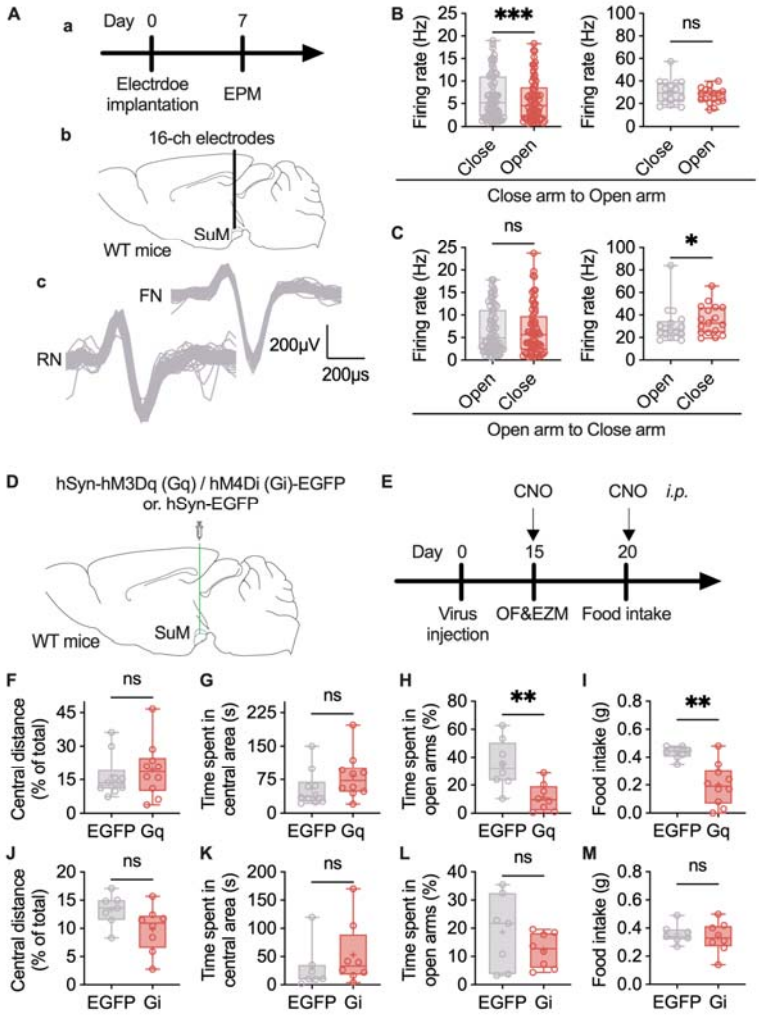

Figure 2. The supramammillary nucleus encodes anxiety-like behavior

(A) Workflow of multi-channel recording (a); electrodes implantation (b) and representative spikes acquired by multi-channel recording (c).

(B) Statistical comparison of the firing rate of RNs (Left) and FNs (Right) while mice transiting from closed arms to open arms. n = 70 RNs and n = 17 FNs per group, Wilcoxon matched-pairs test.

(C) Statistical comparison of the firing rate of RNs (Left) and FNs (Right) while mice transiting from the open arms to closed arms. n = 70 RNs and n = 17 FNs per group, Wilcoxon matched-pairs test.

(D-E) Virus injection information and workflow of chemogenetic manipulation.

(F-G) Statistical comparison of the central distance (F) and the time that mice spent in the central area (G) in OF. n = 10 per group, unpaired t-test for (F) and Mann-Whitney test for (G).

(H) Statistical comparison of the time that mice spent in open arms of EZM. n = 8 per group, unpaired t-test.

(I) Statistical comparison of the consumption of sucrose pellets. n = 8-10 per group, Mann-Whitney test.

(J-K) Statistical comparison of the central distance (J) and the time that mice spent in the central area (K) in OF. n = 7-8 per group, unpaired t-test for (J) and Mann-Whitney test for (K).

(L) Statistical comparison of the time that mice spent in open arms of EZM. n = 7-8 per group, unpaired t-test.

(M) Statistical comparison of the consumption of sucrose pellets. n = 7-8 per group, unpaired t-test. Data in B, C and F-M are presented as Mean ± SEM. "ns"p >0.05, "*"p <0.05, "**"p <0.01, "***"p < 0.001. Also see **Supplemental Figure 2.**

3. Observation of the foot-shock tagged engram cells in SuM

We then tested if there is an ensemble encoding stress and controlling the expression of anxiety. By cross-breeding Fos 2A-iCreER(TRAP2) and Rosa26-LSL-tdTomato (Ai14) mice strain, we acquired TRAP2;Ai14 mouse line to genetically tag and visualize engram cells (Figure 3. A). The foot-shock tagging procedure strongly activated neurons in the SuM but not adjacent areas (Figure 3. B, D). In-situ RNA fluorescent hybridization showed apparent co-localization of the engram cells with Vglut2 (Figure 3. C, E). Almost all SuM cells co-express Vglut2 and Vgat (92.45%). All tagged cells are Vglut2 positive (100%), while only a few co-express Vglut2 and Vgat (13.04%).

The reactivation of SANs was then compared under reward stimulation and stress (Figure 3. F-G). Foot shocks dramatically activated and labeled neurons in SuM (Figure 3. H). Social stress but not reward (present as sucrose pellet here) stimulation-induced neuronal activation (Figure 3. I) and a much higher chance of reactivation of SANs (Figure 3. J). These data suggested the specific regulation of SuM on stress other than reward and the potential existence of the stress-encoding engram cells.

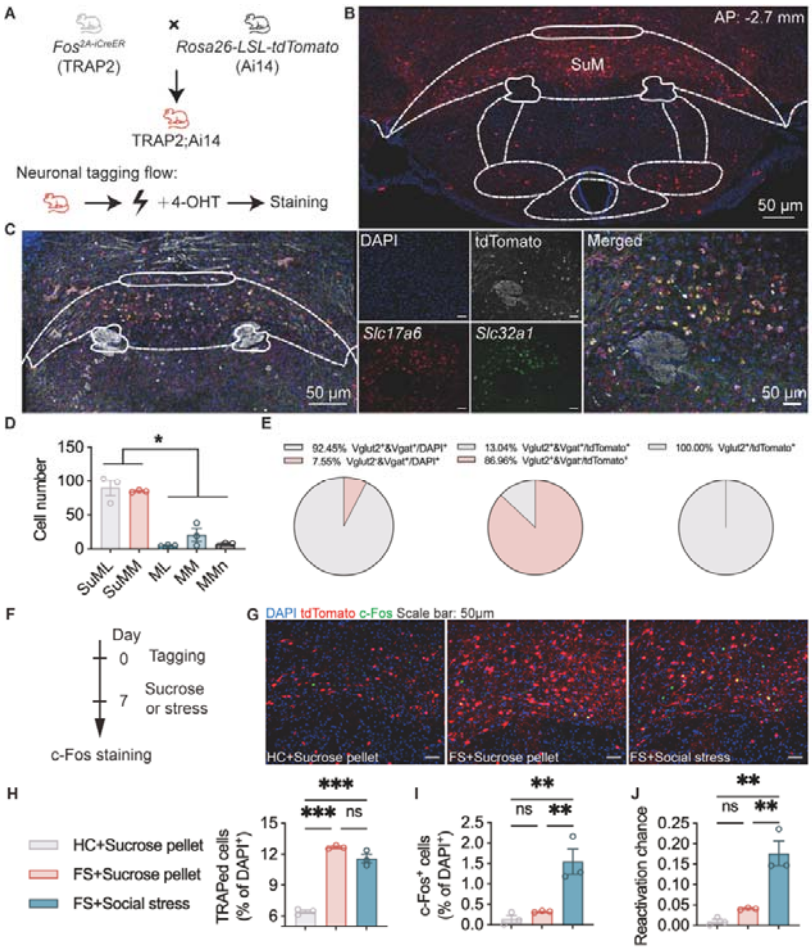

Figure 3. Stress-activated neurons in SuM selectively respond to social stress but not reward

(A) Workflow of mouse breeding and neuronal tagging.

(B) Representative image of stress-tagged cells in SuM (DAPI: blue, tagged cells: red).

(C) Representative images of in situ RNA staining (DAPI: blue, tdTomato: white, Slc17a6: red, Slc32a1: green).

(D) Quantitative statistics of stress-tagged cells in several brain areas. n = 3 per area, one-way ANOVA, Tukey's post-hoc test.

(E) Percentage of co-stain of vglut2, vgat and tdTomato.

(F) Workflow of neuronal tagging and c-Fos staining.

(G) Representative images of stress-tagged cells and c-Fos expression induced by sucrose and social stress (DAPI: blue, tdTomato: red, c-Fos: green).

(H) Statistical comparison of the number of stress-tagged cells in SuM. n = 3 per group, one-way ANOVA, Tukey's post-hoc test.

(I) Statistical comparison of the number of c-Fos^{+} cells after sucrose or social stress exposure. n = 3 per group, one-way ANOVA, Tukey's post-hoc test.

(J) Statistical comparison of the reactivation chance of stress-tagged cells. n = 3 per group, one-way ANOVA, Tukey's post-hoc test. Data in D and H-J are presented as Mean ± SEM. "ns"$p > 0.05$, "*"$p < 0.05$, "**"$p < 0.01$, "***"$p < 0.001$.

4. Reactivation of SuM^{SAN} promotes anxiety-like behavior

Foot-shock stimulation induces persistent memory of fear relevant to the current context. To verify if SANs tagged in SuM regulate fear memory, mice were reintroduced into Context B, which was different from the context in which foot shock was presented. The freezing time was calculated to estimate the retrieved fear memory (Supplemental Figure 3. A). CNO was given 30 minutes before the test, and Gq-activated mice didn't show higher or lower freezing time (Supplemental Figure 3. B). While subjecting to Context A, which is the same as the fear conditioning context, CNO-induced inactivation of SANs didn't alter the freezing of mice (Supplemental Figure 3. C), indicating the non-memory encoding property of SANs in SuM.

Specific activation of the SANs significantly increases the corticosterone (a peripheral indicator of stress) concentration in mouse serum (Figure 4. A-B). Our chemogenetic strategy also showed sound selective activation and inactivation of SANs in SuM (Figure 4. C-F). We then tested if manipulating the SANs of SuM would have any influence on the anxiety-like behavior of mice. Mice were introduced into OF and EZM tests at least 1 week after the tagging of the SANs, followed by reward-seeking tests (Figure 4. G-H). CNO was applied intraperitoneally 30 minutes before the test. Chemogenetic activation of the SANs decreases the total traveled distance of mice in OF and EZM (Supplemental Figure 2. F-G). Mice also showed decreased central distance (Figure 4. I), time spent in the central area of OF (Figure 4. J), time spent in the open arms of EZM (Figure 4. K) and food consumption (Figure 4. L). Unlike the activation manipulation, the inactivation of SANs didn't alter any performance of mice in OF, EZM and reward-seeking tests (Figure 4. M-P, Supplemental Figure 2. H-I). These data suggested that SANs in SuM store anxiety but not fear memory.

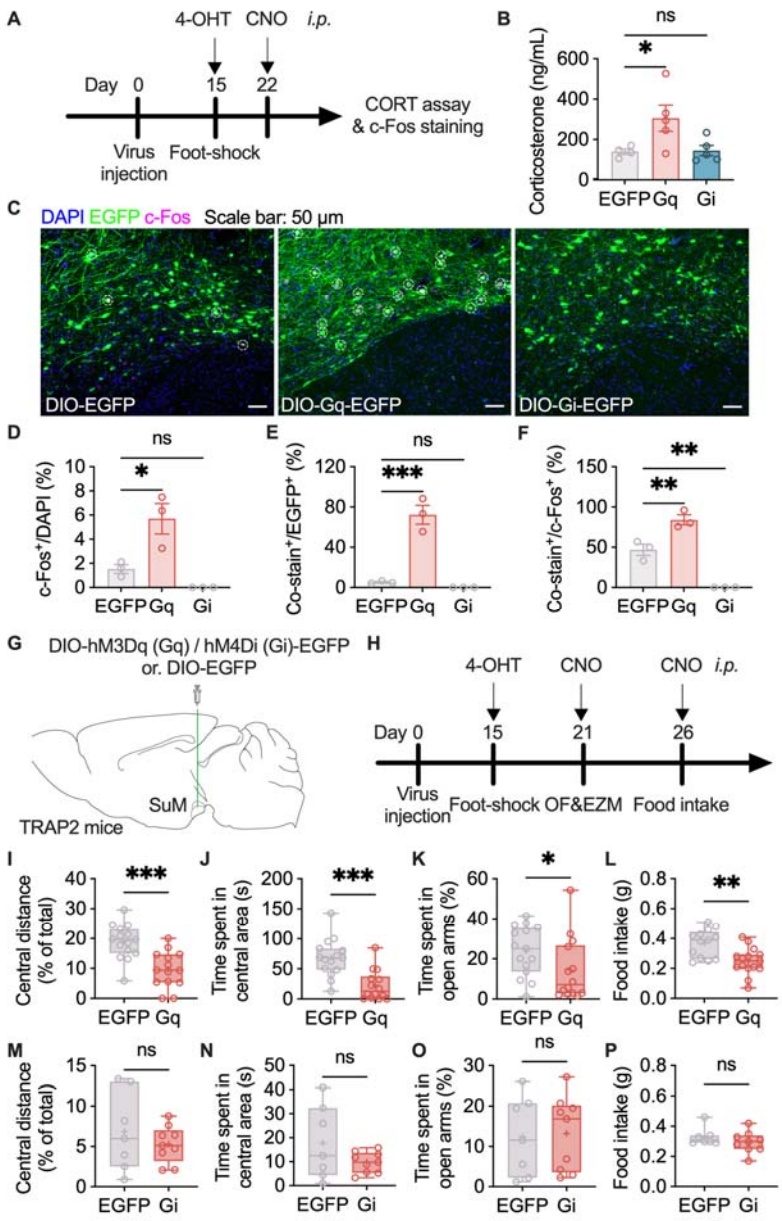

Figure 4. The selected chemogenetic activation of engram cells produces anxiety-like behavior

(A) Workflow of CORT assay and c-Fos staining.

(B) Statistical comparison of serum concentration of corticosterone after applying CNO. n = 4-5 per group, one-way ANOVA, Dunnett's post-hoc test.

(C) Representative images of stress-tagged cells and c-Fos expression induced by chemogenetic manipulation (DAPI: blue, EGFP: green, c-Fos: violet).

(D) Statistical comparison of the percentage of c-Fos$^+$ cells per DAPI in SuM. n = 3 per group, one-way ANOVA, Dunnett's post-hoc test.

(E) Statistical comparison of the percentage of co-stain cells per EGPF$^+$ cells in SuM. n = 3 per group, one-way ANOVA, Dunnett's post-hoc test.

(F) Statistical comparison of the percentage of co-stain cells per c-Fos$^+$ cells in SuM. n = 3 per group,

one-way ANOVA, Dunnett's post-hoc test.

(G-H) Virus injection information and workflow of chemogenetic manipulation.

(I-J) Statistical comparison of the central distance (I) and the time that mice spent in the central area (J) in OF. n = 14-15 per group, unpaired t-test.

(K) Statistical comparison of the time that mice spent in open arms of EZM. n = 14-15 per group, Mann-Whitney test.

(L) Statistical comparison of the consumption of sucrose pellets. n = 13-15 per group, unpaired t-test.

(M-N) Statistical comparison of the central distance (M) and the time that mice spent in the central area (N) in OF. n = 7-9 per group, Mann-Whitney test.

(O) Statistical comparison of the time that mice spent in open arms of EZM. n = 7-9 per group, Mann-Whitney test.

(P) Statistical comparison of the consumption of sucrose pellets n = 7-9 per group, unpaired t-test. Data in B, D-F and I-P are presented as Mean ± SEM. "ns"$p > 0.05$, "*"$p < 0.05$, "**"$p < 0.01$, "***"$p < 0.001$. Also see **Supplemental Figure 2 & Supplemental Figure 3.**

5. vSub-SuM encodes anxiety-like behavior

The SuM receives afferents from variant brain areas, and we therefore looked after this by using a non-virus and virus-based retrograde tracing strategy (Figure 5. A, Supplemental Figure 4. A-C). The dorsal and ventral subiculum afferents were confirmed using CTB-647 and AAV (Supplemental Figure 5. A-B). The projection neurons exclusively express the RNA of the Vglut1 other than the Vgat (Figure 5. B), suggesting that the Sub-SuM projection is an excitatory neuronal projection as the Vglut1 is the crucial marker of glutamatergic neurons. We then tested this in the following electrophysiological experiment. The opto-evoked postsynaptic currents recorded in SuM neurons were blocked by DNQX perfusing, which indicated glutamatergic transmission from Sub to SuM (Figure 5. C-E). To investigate how Sub-SuM projection modulates stress and anxiety-like behavior, we then introduced fiber photometry of calcium concentration to reveal the activity pattern of projection neurons (Figure 5. F-H). The projection neurons in the ventral Sub were more activated when mice moved into the open arms from the closed arms of the EZM, while neurons in the dorsal Sub were not (Figure 5. I-M). When subjecting acute stress events, both dSub- and vSub-SuM projection neurons showed increased calcium activity (Figure 5. N-R). These data suggested the vSub-SuM but not the dSub-SuM may participate in regulating anxiety.

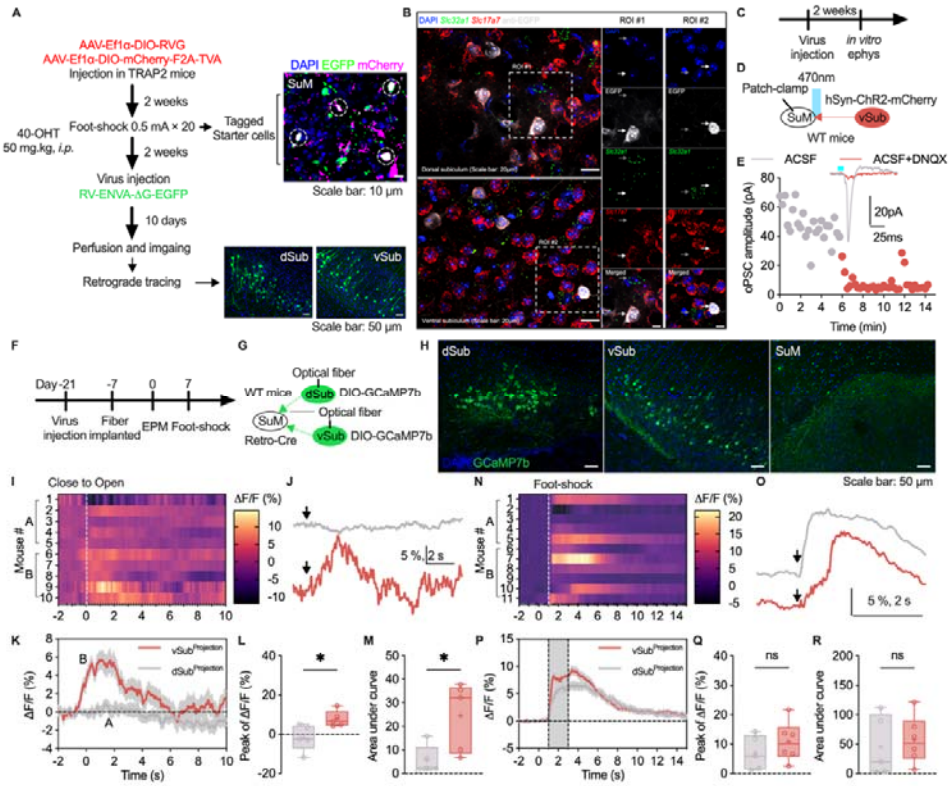

Figure 5. vSub-SuM projection encoding anxiety-like behavior

(A) Workflow of virus-based retrograde neuronal tracing.

(B) Representative images of in situ RNA staining (DAPI: blue, Slc32a1: green, Slc17a7: red, EGFP: white).

(C) Workflow of ex vivo electrophysiological recording.

(D) Schema of optically induced postsynaptic current (oPSC) in SuM.

(E) Representative trace of oPSC.

(F) Workflow of Ca^{2+} imaging.

(G) Schema of Ca^{2+} imaging of dSub and vSub projection neurons.

(H) Representative images of GCaMP7b expression in dSub, vSub and SuM (DAPI: blue, GCaMP7b: green).

(I) Heatmap of Ca^{2+} fluorescent intensity while mice transited from closed to open arms.

(J) Representative Ca^{2+} activity while mice transiting from closed arms to open arms.

(K) Averaged ΔF/F of Ca^{2+} recorded in dSub and vSub.

(L) Statistical comparison of the peak of Ca^{2+} activity. n = 5 per group, unpaired t-test.

(M) Statistical comparison of the area under the curve of Ca^{2+} activity. n = 5 per group, unpaired t-test.

(N) Heatmap of Ca^{2+} fluorescent intensity while mice being exposed to foot-shocks.

(O) Representative Ca^{2+} activity while mice were exposed to foot-shock.

(P) Averaged ΔF/F of Ca^{2+} recorded in dSub and vSub.

(Q) Statistical comparison of the peak of Ca^{2+} activity. n = 5-6 per group, unpaired t-test.

(R) Statistical comparison of the area under the curve of Ca^{2+} activity. n = 5-6 per group, unpaired t-test. Data in L-M and Q-R are presented as Mean ± SEM. "ns"p >0.05, "*"p <0.05. Also see **Supplemental Figure 4** & **Supplemental Figure 5.**

6. Chronic inhibition of vSub-SuM alleviates anxiety-like behavior

After confirming the regulation effect of vSub-SuM on anxiety, this projection was chronically inhibited by applying a chemogenetic strategy. Mice were introduced into the CSDS procedure after specifically expressing Gi protein onto vSub-SuM projection neurons and their axons (Figure 6, A-B, D). The body weight of mice was monitored across the whole procedure to estimate their health status (Figure 6, C). Mice show no change in the social interaction test after CSDS (Figure 6, E). In the EZM test, mice that were inhibited by the activity of vSub-SuM showed less anxiety-like behavior, which was indicated by the longer time spent in the open arms of the EZM, with no significant change of distance traveled (Figure 6, F-G). We then test this by targeting the engram projection of vSub-SuM by specifically inhibiting vSub^{SAN}-SuM (Figure 6, H-K). Notably, mice showed more avoidance of social interaction (Figure 6, L) and less anxiety-like behavior, indicated by the longer time spent in the open arms of the EZM, with no significant change in distance traveled (Figure 6, M-N). These data together suggested that vSub-SuM is the essential neuronal projection that regulates anxiety.

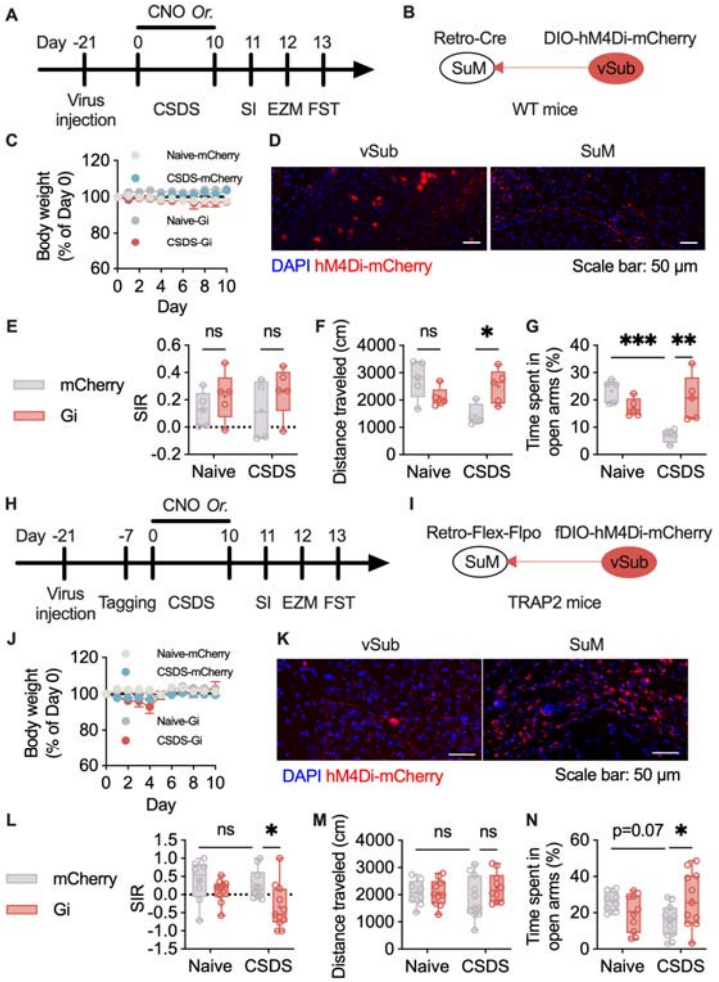

Figure 6. The selective inhibition of vSub-SuM and vSub^{SAN}-SuM alleviated the CSDS-induced anxiety

(A) Workflow of CSDS and chemogenetic manipulation.

(B) Schema of chemogenetic manipulation on specific projection.

(C) Body weight during CSDS.

(D) Representative images of virus expression.

(E) Statistical comparison of social interaction ratio after CSDS. n = 4-5 per group, two-way ANOVA, Sidak's post-hoc test.

(F) Statistical comparison of the distance that mice traveled in EZM. n = 4-5 per group, two-way ANOVA, Sidak's post-hoc test.

(G) Statistical comparison of the time that mice spent in open arms of EZM. Two-way ANOVA, Sidak's post-hoc test.

(H) Workflow of CSDS and chemogenetic manipulation.

(I) Schema of chemogenetic manipulation on specific projection.

(J) Body weight during CSDS.

(K) Representative images of virus expression.

(L) Statistical comparison of social interaction ratio after CSDS. n = 8-11 per group, two-way ANOVA, Sidak's post-hoc test.

(M) Statistical comparison of the distance that mice traveled in EZM. n = 8-11 per group, two-way ANOVA, Sidak's post-hoc test.

(N) Statistical comparison of the time that mice spent in open arms of EZM. Two-way ANOVA, Sidak's post-hoc test. Data in C, E-G, J and L-N are presented as Mean ± SEM. "ns"$p > 0.05$, "*"$p < 0.05$, "**"$p < 0.01$, "***"$p < 0.001$.

Discussion

In this study, we combined multiple methods to determine that the supramammillary nucleus (SuM) is the critical brain region that regulates anxiety. SuM neurons strongly respond to acute and chronic stress, and its activation resulted in robust increased anxiety-like behavior in mice. We then defined a small ensemble of neurons that are activated by stress, called stress-activated neurons (SANs). These SANs specifically respond to stressful stimulation other than reward. Selectively activation of SANs in SuM increased the concentration of serum corticosterone and meanwhile the anxiety-like behavior of mice. Underlying neuronal circuits that may be involved in regulating anxiety were also determined in this study. The subiculum sends glutamatergic projection to SuM and could be activated by stress, while only its ventral part showed the potential effect on the anxiety status transition. We finally determined the inhibition of the SANs in vSub that projecting to SuM is sufficient to alleviate the anxiety of mice after CSDS.

Supramammillary regulation of anxiety

SuM has been demonstrated in response to novel environments, social stimulation(Chen et al., 2020; Cumbers et al., 2007), and stress(Cristina et al., 1993; Escobedo et al., 2023). Given these findings, we assume that SuM may be activated by foot-shock, a quantitative acute stress used in animal models. Consistent with this hypothesis, we found that SuM robustly positively responds to both acute and chronic stress by the observable increase of c-Fos expression, Ca^{2+} concentration in the neuronal body and increased neuronal firing rate. The activation of SuM was also demonstrated to be essential to maintain arousal status(Liang et al., 2023; Pedersen et al., 2017). Sensitization to stressful events and high arousal are often associated with anxiety(Leduke et al., 2023). Thus, our data strongly suggests SuM's potential modulation of anxiety. To further confirm if SuM participates in anxiety regulation, we

recorded neuronal action potential using multi-channel extracellular recording while mice were moving in the elevated plus maze, a traditional model for anxiety test of rodents. Modified neuronal activity frequency while mice transit across open and closed arms supports the idea that SuM may somewhat modulate anxiety. We then manipulated the neuronal activity in SuM using the chemogenetic method and tested mice in EZM, an improved model for anxiety tests of rodents. Decreased exploration time of open arms, indicating an increasing anxiety of mice in which SuM was activated by hM3Dq. We noted that this result is in contrast to some previous reports. Some studies reported that the lesion of SuM and its adjacent areas decreased the anxiogenic behavior in rats(Aranda et al., 2006; Beck' & Fibiger, 1995; Pan & McNaughton, 2002). López-Ferreras et al. used open field, a complicated testing model, and found that the chemogenetic activation of neurons in SuM results in more anxiety-like behaviors in rats(López-Ferreras et al., 2019, 2020). However, further experiments involving specific testing models (e.g., EZM) are needed to confirm if there is a potential difference across species.

Anxiety engram in SuM

Recent studies have raised the importance of activity-tagged neuronal ensemble in regulating various behaviors, particularly memory(Lacagnina et al., 2019; Liu et al., 2012; X. Sun et al., 2020; Tonegawa et al., 2018), food consumption(H. Sun et al., 2023), inflammation reaction(Koren et al., 2021) and emotion(T. R. Zhang et al., 2019; Zheng et al., 2024). Negative experience-related neuronal ensemble in the hippocampus was found to enhance the susceptibility to chronic stress(T. R. Zhang et al., 2019). A most recent article reported that the lateral habenula has a small population of neurons that would be recruited by stress and mediated the development of depression in mice(Zheng et al., 2024). These studies suggest the possibility that SANs are critical for emotional regulation. In this study, we found that SuM was more strongly activated by acute stress than its adjacent areas. These SANs were more likely to be reactivated by following social stress than sucrose reward, showing specific encoding potential of anxiety. As a classic stress-induced symbol of anxiety in the peripheral nervous system, serum corticosterone concentration usually be used to estimate if the individual is anxious. Our data showed that the chemogenetic activation of SANs in SuM increased the serum corticosterone concentration, while inactivation had no effect. Combined with the results of OF, EZM, and contextual fear memory tests, we can conclude that the SANs we identified in SuM only store information about stress other than memory. We also found that both the non-selective activation of SuM neurons and selective activation of SANs in SuM significantly suppressed the consumption of sucrose pellets. This result may be attributed to the anxiety-induced suppression of reward-seeking(Peng et al., 2021). However, further experiments are still needed to confirm whether this effect is anxiety-dependent and if basal food consumption would be affected.

A relevant neural circuit that regulates anxiety

The supramammillary nucleus recruits and is recruited in neuronal projections with the hippocampus, medial septum, and cortex(Kesner et al., 2023). To further understand the underlying circuitry mechanism of the supramammillary regulation of anxiety, we determined two projections from the dorsal part of the subiculum (dSub) and ventral part of the subiculum (vSub) to SuM(Tang et al., 2016). Fiber photometry measurement of Ca^{2+} concentration of projecting neurons in dSub and vSub revealed the encoding role of

vSub-SuM other than dSub-SuM based on the increased Ca^{2+} activity while mice transiting from the closed arms to the open arms. To confirm the vSub-SuM regulation of anxiety, we introduced the CSDS model and found that the constant inhibition of vSub-SuM activity significantly abolished the CSDS-induced anxiety in mice. Consistent with this result, selective inhibition of $vSub^{SAN}$-SuM was also sufficient to alleviate anxiety. Unlike the dorsal hippocampal regulation of cognition, the ventral hippocampus often shows its regulation of emotion(Shi et al., 2023). The Ventral CA1 area and its projection to the lateral hypothalamic area were found to mediate innate anxiety, and its activation increased anxiety-like behavior in mice(Jimenez et al., 2018). Although very close, neurons in the subiculum are pretty different from those in CA1(Aggleton & Christiansen, 2015; Ding et al., 2020). vSub and its downstream brain areas were found to regulate anxiety(Ghasemi et al., 2022; Mueller et al., 2004). Jing-Jing et al. reported that vSub and its projection to the anterior hypothalamic nucleus is essential for anxiety because the inhibition of this projection decreases the anxiety-like behavior(Yan et al., 2022). Our data is consistent with these findings and suggests the mediation role of vSub and its projections to different subareas in the hypothalamus.

In conclusion, activation of SuM increases anxiety-like behavior. A neuronal ensemble activated by stressful events stores anxiety but not memory. Activation of these SANs also significantly increases anxiety-like behavior and suppresses reward-seeking. SuM receives glutamatergic projection from vSub, and inhibition of this projection can diminish the CSDS-induced anxiety. These results suggest that stress may leave engram-like traces in the brain, and its activation results in anxiety.

Acknowledgment

We thank Dr. Wenting Wang for his generous gift of transgenic mice. We thank all the members of MTT for their valuable comments.

This research was funded by the National Natural Science Foundation of China (No. 82371518, No. 82071516), STI 2030-Major Projects 2021ZD0200500, Humanities and Social Science Fund of Ministry of Education of China (No. 22XJC880005), Innovation Capability Support Program of Shaanxi (Program No. 2021PT-055), Natural Science Basic Research Plan in Shaanxi Province of China (Program No. 2024JC-YBQN-0902), and Scientific and Technological Innovation Team of Shaanxi Innovation Capability Support Plan (2022TD-47).

Declaration of interests

The authors declare no competing interests.

Methods

Animal

Male C57BL6/J mice aged from 12 - 20 weeks were used. $Fos^{2A\text{-}iCreER}$ (TRAP2) mice were a gift from Wenting Wang (JAX, Cat. 030323). Rosa26-CAG-LSL-tdTomato (Ai14) mice were purchased from the Shanghai Model Organisms Center (Cat. NM-KI-225042). Male CD-1 mice aged 8-10 months were purchased from Charles River (Cat. 201). To construct the TRAP2;Ai14 mouse line, homozygous male TRAP2 and homozygous female Ai14 were bred. Homozygous TRAP2;Ai14 mouse line was maintained and used in experiments. We performed genotyping for TRAP2 and Ai14 using PCR with the following primers. For TRAP2 (Wild-type: 357 bp, Mutant: 232 bp), wild-type forward: GTCCGGTTCCTTCTATGCAG, mutant forward: CCTTGCAAAAGTATTACATCACG, common: GAACCTTCGAGGGAAGACG; for Ai14 (Wild-type: 297 bp, Mutant: 196 bp), wild-type forward: AAGGGAGCTGCAGTGGAGTA, wild-type reverse: CCGAAAATCTGTGGGAAGTC, mutant forward: GGCATTAAAGCAGCGTATCC, mutant reverse: CTGTTCCTGTACGGCATGG.

Mice were reared in a constant temperature and humidity environment (22 ± 1 °C, 30-40% RH) on a scale of 4-5 per cage, and the indoor day and night cycle was controlled by a fixed intensity light source (Turn on time 08:00-20:00). Each mouse was acclimated for 1-2 min. This procedure lasted for three days before the behavioral experiments. Mice were fed ad libitum and euthanized using CO_2 after finishing all tests. The experimental protocols described here were approved by the Animal Ethics Committee of Shaanxi Normal University.

Behavioral procedure

Acute stress

We used a previously reported acute stress procedure(Marcus et al., 2020), which consisted of 20 foot-shocks at the intensity of 0.5 mA and randomly distributed across 10 minutes. Foot-shocks were delivered by the fear conditioning box (Med-associates).

Chronic stress

We used chronic social defeat stress (CSDS) as the chronic stress procedure to induce anxiety and depression in mice(Kim et al., 2017). One C57BL6/J mouse would live with one CD-1 mouse in the homecage separated by a transparent plexiglass board with several small holes. Mice were allowed to contact each other directly for 10 minutes. This operation was repeated every day for 10 days. The body weight was inspected and recorded every day before contacting.

Open field

Open field (OF) test was carried out in a 50 × 50 × 35 cm arena made of white plexiglass. Mice were allowed to move freely in the arena for 10 minutes, and the distance mice moved and the time mice spent in the central area were recorded and analyzed.

Elevated plus maze

Elevated plus maze (EPM) consists of two open arms (30 × 7 cm), two closed arms (30 × 7 × 14 cm) and a central area (7 × 7 cm). Mice were allowed to move freely in the arena for 10 min, and the time mice spent in open arms was recorded and analyzed.

Elevated zero maze

Elevated zero maze (EZM) was used to test whether mice were anxious. The EZM used in this study was made of organic glass (at a height of 60 cm), with an inner diameter of 51.8 cm and an outer diameter of 65 cm. The closed arms of the EZM are separated by two 15 cm-high organic glasses, the outer one of which is opaque. After a 15-minute habituation to the room, mice were put into the EZM and allowed to move freely for 10 minutes. The video was collected and analyzed using EthovisionXT. The time that mice spent in the open arms were compared between groups to evaluate anxiety-like behavior.

Reward-seeking

On the first day, sucrose pellets were provided for habituation feeding. Mice were then deprived of food on the second day. On the third day, mice were put into a new homecage without bedding and allowed to eat freely for 2 hours. Pellets were weighted to evaluate if the experimental manipulation influenced the reward-seeking of mice.

Social interaction test

The social interaction test (SIT) used in this study was conducted as previously described(Kim et al., 2017). The SIT is composed of two 2.5-minute phases. In the first phase (No-target), we put the C57 mouse into the periphery side of the arena opposite the social interaction area (SIA). We allowed it to explore the arena freely. In the second phase (With-target), the C57 mouse was introduced to the arena again with a new CD-1 mouse in the SIA. The social interaction ratio (SIR) was calculated using the following formula:

$$Social\ interaction\ ratio\ (SIR) = \frac{Time\ in\ SIA^{With-target} - Time\ in\ SIA^{No-target}}{Time\ in\ SIA^{With-target} + Time\ in\ SIA^{No-target}}$$

Contextual fear conditioning

Contextual fear memory was examined using contextual fear conditioning (CFC) as previously described(Chang et al., 2022; J. Zhang et al., 2024). Mice were allowed to habituate the fear conditioning box (MED-VFC-USB-M, Med associates) for 10 minutes (Day 1, Context A). Mice were allowed to explore the box freely for 4 minutes at the beginning of the learning phase (cumulative freezing time during this phase was set as the baseline). Then, three foot-shock (0.75 mA, 2 s) were delivered at 4, 6.25, and 8.5 minutes after the beginning of the experiment. Ninety seconds after the last foot shock, the mice were transferred back to the homecage. Mice were returned to Context A on the fifth day to test the "Loss of function" of the engram cells with CNO injection 30 minutes before video recording. Mice were returned to Context B on the fifth day to test the "Gain of function" of the engram cells with CNO injection 30 minutes before video recording. Video was collected and analyzed using VideoFreeze software, a commercial software provided by Med-associates.

Neuronal tagging of stress-activated neurons

To specifically label stress-activated neurons (SANs), TRAP2 or TRAP2;Ai14 mice received intraperitoneally (i.p.) injection with 4-Hydroxytamoxifen (4-OHT, 50 mg/kg) immediately after acute stress or the learning phase of CFC. Mice were introduced into the next experiment or test in 7 days to allow Cre-dependent recombination.

4-OHT (CAS No. 68392-35-8. Sigma, Cat. H6278 or Bidepharm, Cat. BD00958757) was dissolved in DMSO at 62.5 mg/mL and diluted with vehicle (containing 10 %

TWEEN-80 and 80 % saline) in the tagging day. The final concentration of DMSO was kept below 10 % to avoid toxicity.

Observation of the reactivation of SANs

One week after neuronal tagging, TRAP2;Ai14 mice were introduced into the following procedure to test if the previously tagged SAN will be reactivated when suffering social stress. Mice were divided into three groups: mice in the first group were home-cage-tagged, and the c-Fos expression was induced by sucrose pellets; mice in the second group were foot-shock-tagged, and the c-Fos expression was induced by sucrose pellets; mice in the third group were foot-shock-tagged, and the c-Fos expression was induced by social stress (one CD-1 mice were put into the home-cage). Mice were then sacrificed into c-Fos staining using immunofluorescence 90 minutes after sucrose pellets feeding or social stress. The number of the c-Fos positive neurons was counted to estimate if reward and cross-strain social stress could activate the neurons in SuM. The reactivation chance of SAN was calculated using the following formula:

$$Reactivation\ chance\ (\%) = (c - Fos^{+}/DAPI^{+}) \times (tdTomato^{+}/DAPI^{+}) \times 100$$

Viral vector

Adeno-associated virus (AAV) was used to label and manipulate specific neurons or inspect calcium concentration. To manipulate the activity of the SAN in SuM, AAV2/9-hSyn-DIO-hM3Dq/hM4Di-EGFP (titer: 5.00E+12 μg/, BrainVTA, Cat. PT-0891 & PT-0344) and its control vector AAV2/9-hSyn-DIO-EGFP (titer: 5.00E+12 μg/mL, BrainVTA, Cat. PT-1103) were injected into SuM of TRAP2 mice respectively.

To chronically inhibit vSub-SuM circuitry activity, AAV2/Retro-hSyn-Cre (titer: 2.00E+12 μg/mL, Taitool, Cat. S0278) was injected into SuM, AAV2/9-hSyn-DIO-hM4Di-mCherry (titer: 2.00E+12 μg/mL, Taitool, Cat. S0193) and its control vector AAV2/9-hSyn-DIO-mCherry (titer: 2.00E+12 μg/mL, Braincase, Cat. BC-0025) were injected into vSub of wild-type mice.

To chronically inhibit $vSub^{SAN}$-SuM circuitry activity, AAV2/Retro-CAG-Flex-Flpo (titer: 2.00E+12 μg/mL, Taitool, Cat. S0273) was injected into SuM, AAV2/9-EF1α-fDIO-hM4Di-mCherry (titer: 2.00E+12 μg/mL, Taitool, Cat. S0336) and its control vector AAV2/9-hSyn-fDIO-mCherry (titer: 2.00E+12 μg/mL, BrainVT, Cat. PT-0341) were was injected into vSub of TRAP2 mice.

AAV2/9-hSyn-GCaMP7b (titer: 5.00E+12 μg/mL, BrainVTA, Cat. PT-2708) was injected into SuM of wild-type mice to inspect the calcium concentration using fiber photometry.

To inspect the calcium concentration of vSub-SuM projection neurons, AAV2/Retro-hSyn-Cre (titer: 2.00E+12 μg/mL, Taitool, Cat. S0278) was injected into SuM and AAV2/9-hSyn-DIO-GCaMP7b (titer: 5.00E+12 μg/mL, BrainVTA, Cat. PT-2892) was injected into vSub of wild-type mice.

For the ex vivo electrophysiological experiment, AAV2/9-hSyn-ChR2-mCherry (titer: 5.00E+12 μg/mL, BrainVTA, Cat. PT-0150) was injected into vSub of wild-type mice.

Neuronal tracing

Initial retrograde neuronal tracing was performed using serotype-2 AAV

(AAV2/Retro-hSyn-EGFP, titer: 5.00E+12 μg/mL, Taitool, Cat. S0237) and CTB-647 (1 μg/μL, ThermoFisher, Cat. C34778). They were injected into SuM of wild-type mice. Mice were then sacrificed and the brain was cut into coronal slices for imaging in 2 weeks.

To precisely trace the neuronal afferents to SuM^{SAN}, AAV2/9-Ef1α-DIO-RVG (titer: 5.00E+12 μg/mL, BrainVTA, Cat. PT-0061) and AAV2/9-Ef1α-DIO-mCherry-F2A-TVA (titer: 5.00E+12 μg/mL, BrainVTA, Cat. PT-0207) were injected into SuM of TRAP2 mice simultaneously. And the rabis virus (RV) RV-ENVA-ΔG-EGFP (titer: 2.00E+08 IFU/mL, BrainVTA, Cat. R01001) was injected into SuM in 2 weeks after neuronal tagging. Mice were then sacrificed and the brain was cut into coronal slices for imaging in 2 weeks.

Stereotype surgery

Mice were anesthetized using isoflurane at a concentration of 1.5 ~2.0 %. Virus was injected into SuM (AP: -2.8, ML: 0, DV: -4.5 mm), dSub (AP: -2.8, ML: ±0.7, DV: -1.7 mm) or vSub (AP: -3.5, ML: ±3.0, DV: -4.6 mm) depends on experimental design. If only one type of virus is needed in a single brain area, the given final volume is typically 150 nL. Otherwise the given final volume of mixed virus solution was 200 nL at the injection velocity of 50 nL/min. The syringe was held in that position for at least 5 minutes and carefully removed from the brain. Mice were then returned to their homecage with health inspection for the following consecutive days. All mice that experienced surgery were introduced into the next experiment in 2 weeks or more to allow virus expression.

For fiber photometry, ceramic ferrule (Outer diameter: 2.5 mm, Core diameter: 0.2 mm, NA: 0.50) was inserted into SuM (AP: -2.8, ML: 0, DV: -4.3 mm), dSub (AP: -2.8, ML: ±0.7, DV: -1.5 mm) or vSub (AP: -3.5, ML: ±3.0, DV: -4.4 mm) in 2 weeks after receiving virus injection under the guidance of laser (wavelength: 470 nm). Calcium imaging was conducted at least 1 week after ferrule implementation.

Fiber photometry

Commercial equipment (Thinker Tech) was used to inspect the calcium concentration. Fluorescence activated by the laser at 470 nm, which is transmitted through a low-autofluorescence fiber-optic patch cord and rotary (Doric lenses) and collected. The final activation intensity was set to ~40 μW. The sampling rate was 50 Hz across all recordings. Mice were habituated with the fiber-optic patch cord connection procedure for consecutive 3 days before recording. A TTL lasting 0.1 seconds was given to the control software to mark the event before each foot-shock (Med-associates), or while mice moved from the closed arms to the open arms in EPM (USB-IO box, Noldus). Continuous data was stored as a *.tdms file and analyzed using customer-made software based on MATLAB.

Chemogenetic manipulation

To manipulate the neuronal activity of SuM in wild-type and TRAP2 mice, Clozapine N-oxide (CNO, 5 mg/kg; Cayman, Cat. 25780) was injected i.p. 30 minutes before the behavioral test. While performing chronic inhibition of circuitry activity, CNO was delivered through oral application (0.025 mg/mL).

For acute and chronic experiments, CNO was dissolved in DMSO at 10 mg/mL and stored at -20 □ or in saline at 1 mg/mL and stored at -80 □, respectively. The storage solution was diluted with saline to 0.75 mg/mL for acute manipulation and 0.025 mg/mL for chronic inhibition as a working solution on the experiment day.

Immunofluorescence

Mice were anesthetized using 20 % urethane and perfused with PBS or saline. The mouse brain was dissected and immersed in 4 % paraformaldehyde (PFA) at 4 □ overnight. The PFA solution can then be replaced with a 30 % sucrose solution. After sinking to the bottom, the brain was embedded with optimal cutting temperature compound (OCT) and frozen in a cryostat microtome (CM1950, Leica). 40 µm coronal slices were cut and collected in a 24-well plate. After washing out the residual OCT with PBS, slices were blocked in 0.3 % tritonX-100 and 10 % normal donkey serum at room temperature (RT) for 2 hours. Slices were then incubated in primary antibody dilution (Rabbit anti-c-Fos, 1:500, Cell Signaling Technology, Cat. 2250) at 4 □ overnight. The next day, slices were washed and incubated in secondary antibody dilution (Donkey anti-rabbit with AF647, 1:500, JacksonImmunoResearch, Cat. 706-605-148) at RT for 2 hours. After washing, slices were transferred to slides and mounted with an antifade reagent (ThermoFisher, Cat. P36981). Images of slices were collected using a Zeiss M2 microscope and then analyzed.

Fluorescent in-situ hybridization of RNA

Handle sample as described in the *Immunofluorescence* section. 10 µm slices were cut and dried at RT for ~15 minutes and then baked at 37 □ for 30 minutes in the hybridization oven. The baked slides were then moved to a pre-cooled 4 % PFA solution for fixation (~15 minutes). The slices were dehydrated in 100 % ethanol at RT for 5 minutes. Repeat the dehydration step. The following steps were performed as described in the manufacturer's operation manual (ACDbio, Cat. 323100). To label the RNA of vglut1, vglut2 and vgat, slices were hybridized with Mm-*Slc17a7* (ACDbio, Cat. 416631-C1), Mm-*Slc17a6* (ACDbio, Cat. 319171-C1) and Mm-*Slc32a1* (ACDbio, Cat. 319191-C3) respectively. And then stained using Opal dyes.

Co-stain of protein and RNA

After confirming the positive stain of RNA, slices were blocked in 10 % normal goat serum for 1 hour. Remove the blocking solution and incubate the slices with primary antibody dilution (Mouse anti-GFP, 1:500, ThermoFisher, Cat. MA5-16256; Rabbit anti-tdTomato, 1:500, Oasis Biofarm, Cat. OB-PRB013) at 4 □ overnight. Wash slides using PBS and incubate slides in secondary antibody solution (Goat anti-rabbit/mouse, HRP. Proteintech, Cat. PR30009) at RT for 1 hour (avoid light). After washing, slices were stained using Opal dye at RT for 30 minutes. Slides were then mounted and imaged.

Corticosterone assay

The mice's whole blood was collected 90 minutes after CNO injection (5 mg/kg, i.p.). Samples were centrifuged at 2000×g for 10 minutes at 4 □ after leaving to stand at RT for 30-60 minutes. The supernatant fluid was then carefully collected as the serum. According to the manufacturer's operation manual, the corticosterone assay was then performed using a commercial Elisa kit (Beyotime, Cat. PC100).

***Ex vivo* Electrophysiology**

Mice were anesthetized with urethane and then decapitated. The brain was quickly removed from the skull and immersed in pre-cooled sucrose-based cutting solution (in mM, 225 sucrose, 2.5 KCl, 1.25 NaH_2PO_4, 26 $NaHCO_3$, 11 D-Glucose, 5 L-Ascorbic Acid, 3 Sodium Pyruvate, 7 $MgSO_4 \cdot 7H_2O$, 0.5 $CaCl_2$). After being fixed on a metal pallet, the brain

was cut into 300-μm slices. Slices were then collected and incubated in artificial cerebrospinal fluid (ACSF) containing (in mM): 122 NaCl, 2.5 KCl, 1.25 NaH_2PO_4, 26 $NaHCO_3$, 11 D-Glucose, 2 $MgSO_4 \cdot 7H_2O$, 2 $CaCl_2$ equilibrated with 95% O_2-5% CO_2 at 28 □ for at least 1 hour before recording.

To evoke postsynaptic current (PSC) using light, whole-cell recording was made on the neurons near the axons illuminated by ChR2-mCherry injected in vSub. The final light intensity on the end of the optical fiber was set to ~5 mW/mm^2. Then the blue light (470 nm, width: 10 ms, frequency: 0.05 Hz) was given to evoke specific optical-PSC (oPSC). DNQX (20 μM) was perfused into the ACSF to extract the AMPA-dependent current from the raw oPSCs after establishing a 5-minute baseline.

***In vivo* Electrophysiology**

Mice were anesthetized with 2% isoflurane and held on a stereotype. Sixteen-channel microwire array electrodes (KD-MWA, KedouBC), a 4x4 array of 25 μm NiTi wire spaced 200 μm, were slowly inserted into the mouse brain. Four small nails were first inserted into the skull, with a ground wire pre-soldered onto one of them. The electrode was left at the SuM (AP: -2.8, ML: 0, DV: -4.55 mm), and then dental cement was used to fix it onto the skull.

Mice were introduced to the recording arena at least one week after surgery. During the day, the electrode on the mouse skull was connected to the OpenEphys acquisition board through an Intan head stage. OpenEphys GUI was used to visualize and save electrical signals. Mice were allowed to move freely inside a homecage-like arena for at least 20 minutes. Only data acquired during the last 5 min were saved and then analyzed by Python-based software and a customized Python script.

Spikes were detected and divided into single units using the SpikeInterface (https://github.com/SpikeInterface/spikeinterface). Continuous binary raw data (sampling rate: 30 kHz) were imported and filtered using a bandpass butter filter at a cutoff value of 300 Hz. Movement artifacts were removed by subtracting medians over all channels. Templates were then extracted and fitted using spyking-circus2 inside the SpikeInterface frame. Neurons meeting the following criteria were excluded from the following analysis: (1) spikes with refracting period violations smaller than 1 ms, accounting for more than 2 % of total spikes, and (2) total frequency lower than 0.2 Hz. Neurons with spike frequency ≥ 10 Hz were clustered as regular-spiking neurons (RN), while those < 10 Hz were fast-spiking neurons (FN) according to a previous study(Chen et al., 2020). Local field potential was extracted and analyzed using the power spectrum analysis tool in MATLAB.

Statistical analysis

Data are presented as the mean ± SEM in all figures in this manuscript. In terms of the normally distributed data and equal standard deviation, the independent t-test for unpaired data and the dependent t-test for paired data were performed in GraphPad software to compare mean values between the two groups. Otherwise, the Mann□Whitney test for unpaired data and the Wilcoxon test for paired data were performed instead. One-way ANOVA followed by Tukey's post-hoc test and two-way ANOVA followed by Sidak's post hoc test were performed to compare mean values among more than three groups. The *p*-value, which is smaller than 0.05 was considered as indicating a statistical significance between

groups. “*” represents $p < 0.05$, “**” represents $p < 0.01$, “***” represents $p < 0.001$.

References

Aggleton, J. P., & Christiansen, K. (2015). The subiculum: The heart of the extended hippocampal system. *Progress in Brain Research*, *219*, 65–82. https://doi.org/10.1016/bs.pbr.2015.03.003

Aranda, L., Santín, L. J., Begega, A., Aguirre, J. A., & Arias, J. L. (2006). Supramammillary and adjacent nuclei lesions impair spatial working memory and induce anxiolitic-like behavior. *Behavioural Brain Research*, *167*(1), 156–164. https://doi.org/10.1016/j.bbr.2005.09.002

Azevedo, E. P., Pomeranz, L., Cheng, J., Schneeberger, M., Vaughan, R., Stern, S. A., Tan, B., Doerig, K., Greengard, P., & Friedman, J. M. (2019). A Role of Drd2 Hippocampal Neurons in Context-Dependent Food Intake. *Neuron*, *102*(4), 873-886.e5. https://doi.org/10.1016/j.neuron.2019.03.011

Beck', C. H. M., & Fibiger, H. C. (1995). Conditioned Fear-induced Changes in Behavior and in the Expression of the Immediate Early Gene c-fos: With and Without Diazepam Pretreatment. *The Journal of Neuroscience*, *15*(l), 709–720. https://doi.org/10.1523/JNEUROSCI.15-01-00709.1995

Chang, Y., Zhang, J., Zhang, J., Zhu, W., Zheng, Q., Qian, Z., Wei, C., Liu, Y., Liu, Z., Ren, W., & Han, J. (2022). N6-methyladenosine RNA modification of glutamatergic neurons is associated with contextual fear discrimination. *Physiology and Behavior*, *248*(February), 113741. https://doi.org/10.1016/j.physbeh.2022.113741

Chen, S., He, L., Huang, A. J. Y., Boehringer, R., Robert, V., Wintzer, M. E., Polygalov, D., Weitemier, A. Z., Tao, Y., Gu, M., Middleton, S. J., Namiki, K., Hama, H., Therreau, L., Chevaleyre, V., Hioki, H., Miyawaki, A., Piskorowski, R. A., & McHugh, T. J. (2020). A hypothalamic novelty signal modulates hippocampal memory. *Nature*, *586*(7828), 270–274. https://doi.org/10.1038/s41586-020-2771-1

Cristina, M., Silveira, L., Sandner, G., & Graeff, F. G. (1993). Induction of Fos immunoreactivity in the brain by exposure to the elevated plus-maze. *Behavioural Brain Research*, *56*, 115–118. https://doi.org/10.1016/0166-4328(93)90028-o

Cumbers, M. R., Chung, S. T., & Wakerley, J. B. (2007). A neuromodulatory role for oxytocin within the supramammillary nucleus. *Neuropeptides*, *41*(4), 217–226. https://doi.org/10.1016/j.npep.2007.04.004

Ding, S. L., Yao, Z., Hirokawa, K. E., Nguyen, T. N., Graybuck, L. T., Fong, O., Bohn, P., Ngo, K., Smith, K. A., Koch, C., Phillips, J. W., Lein, E. S., Harris, J. A., Tasic, B., & Zeng, H. (2020). Distinct Transcriptomic Cell Types and Neural Circuits of the Subiculum and Prosubiculum along the Dorsal-Ventral Axis. *Cell Reports*, *31*(7).

https://doi.org/10.1016/j.celrep.2020.107648

Escobedo, A., Holloway, S. A., Votoupal, M., Cone, A. L., Skelton, H., Legaria, A. A., Ndiokho, I., Floyd, T., Kravitz, A. V., Bruchas, M. R., & Norris, A. J. (2023). Glutamatergic supramammillary nucleus neurons respond to threatening stressors and promote active coping. *ELife*, *12*. https://doi.org/10.7554/eLife.90972

Fanselow, M. S., & Dong, H. W. (2010). Are the Dorsal and Ventral Hippocampus Functionally Distinct Structures? In *Neuron* (Vol. 65, Issue 1, pp. 7–19). https://doi.org/10.1016/j.neuron.2009.11.031

Farrell, J. S., Lovett-Barron, M., Klein, P. M., Sparks, F. T., Gschwind, T., Ortiz, A. L., Ahanonu, B., Bradbury, S., Terada, S., Oijala, M., Hwaun, E., Dudok, B., Szabo, G., Schnitzer, M. J., Deisseroth, K., Losonczy, A., & Soltesz, I. (2021). Supramammillary regulation of locomotion and hippocampal activity. *Science*, *374*, 1492–1496. https://doi.org/10.1126/science.abh4272

Forro, T., Volitaki, E., Malagon-Vina, H., Klausberger, T., Nevian, T., & Ciocchi, S. (2022). Anxiety-related activity of ventral hippocampal interneurons. *Progress in Neurobiology*, *219*. https://doi.org/10.1016/j.pneurobio.2022.102368

Ghasemi, M., Navidhamidi, M., Rezaei, F., Azizikia, A., & Mehranfard, N. (2022). Anxiety and hippocampal neuronal activity: Relationship and potential mechanisms. *Cognitive, Affective and Behavioral Neuroscience*, *22*(3), 431–449. https://doi.org/10.3758/s13415-021-00973-y

Guenthner, C. J., Miyamichi, K., Yang, H. H., Heller, H. C., & Luo, L. (2013). Permanent genetic access to transiently active neurons via TRAP: Targeted recombination in active populations. *Neuron*, *78*(5), 773–784. https://doi.org/10.1016/j.neuron.2013.03.025

Jimenez, J. C., Su, K., Goldberg, A. R., Luna, V. M., Biane, J. S., Ordek, G., Zhou, P., Ong, S. K., Wright, M. A., Zweifel, L., Paninski, L., Hen, R., & Kheirbek, M. A. (2018). Anxiety Cells in a Hippocampal-Hypothalamic Circuit. *Neuron*, *97*(3), 670-683.e6. https://doi.org/10.1016/j.neuron.2018.01.016

Josselyn, S. A., & Tonegawa, S. (2020). Memory engrams: Recalling the past and imagining the future. *Science*, *367*(6473). https://doi.org/10.1126/science.aaw4325

Kesner, A. J., Mozaffarilegha, M., Rajamani, K. T., Arima, Y., Harony-Nicolas, H., Hashimotodani, Y., Ito, H. T., Song, J., & Ikemoto, S. (2023). Hypothalamic Supramammillary Control of Cognition and Motivation. *Journal of Neuroscience*, *43*(45), 7538–7546. https://doi.org/10.1523/JNEUROSCI.1320-23.2023

Kesner, A. J., Shin, R., Calva, C. B., Don, R. F., Junn, S., Potter, C. T., Ramsey, L. A.,

Abou-Elnaga, A. F., Cover, C. G., Wang, D. V., Lu, H., Yang, Y., & Ikemoto, S. (2021). Supramammillary neurons projecting to the septum regulate dopamine and motivation for environmental interaction in mice. *Nature Communications*, *12*(1). https://doi.org/10.1038/s41467-021-23040-z

Kim, H.-D., Call, T., Carotenuto, S., Johnson, R., & Ferguson, D. (2017). Testing Depression in Mice: a Chronic Social Defeat Stress Model. *BIO-PROTOCOL*, *7*(7). https://doi.org/10.21769/bioprotoc.2203

Koren, T., Yifa, R., Amer, M., Krot, M., Boshnak, N., Ben-Shaanan, T. L., Azulay-Debby, H., Zalayat, I., Avishai, E., Hajjo, H., Schiller, M., Haykin, H., Korin, B., Farfara, D., Hakim, F., Kobiler, O., Rosenblum, K., & Rolls, A. (2021). Insular cortex neurons encode and retrieve specific immune responses. *Cell*, *184*(24), 5902-5915.e17. https://doi.org/10.1016/j.cell.2021.10.013

Lacagnina, A. F., Brockway, E. T., Crovetti, C. R., Shue, F., McCarty, M. J., Sattler, K. P., Lim, S. C., Santos, S. L., Denny, C. A., & Drew, M. R. (2019). Distinct hippocampal engrams control extinction and relapse of fear memory. *Nature Neuroscience*, *22*(5), 753–761. https://doi.org/10.1038/s41593-019-0361-z

Leduke, D. O., Borio, M., Miranda, R., & Tye, K. M. (2023). Anxiety and depression: A top-down, bottom-up model of circuit function. *Annals of the New York Academy of Sciences*, *1525*(1), 70–87. https://doi.org/10.1111/nyas.14997

Li, J., Sun, X., You, Y., Li, Q., Wei, C., Zhao, L., Sun, M., Meng, H., Zhang, T., Yue, W., Wang, L., & Zhang, D. (2022). Auts2 deletion involves in DG hypoplasia and social recognition deficit: The developmental and neural circuit mechanisms. *Science Advances*, *8*, 1238. https://doi.org/10.1126/sciadv.abk1238

Li, Y., Bao, H., Luo, Y., Yoan, C., Sullivan, H. A., Quintanilla, L., Wickersham, I., Lazarus, M., Shih, Y. Y. I., & Song, J. (2020). Supramammillary nucleus synchronizes with dentate gyrus to regulate spatial memory retrieval through glutamate release. *ELife*, *9*. https://doi.org/10.7554/eLife.53129

Li, Y. D., Luo, Y. J., Chen, Z. K., Quintanilla, L., Cherasse, Y., Zhang, L., Lazarus, M., Huang, Z. L., & Song, J. (2022). Hypothalamic modulation of adult hippocampal neurogenesis in mice confers activity-dependent regulation of memory and anxiety-like behavior. *Nature Neuroscience*, *25*(5), 630–645. https://doi.org/10.1038/s41593-022-01065-x

Liang, M., Jian, T., Tao, J., Wang, X., Wang, R., Jin, W., Chen, Q., Yao, J., Zhao, Z., Yang, X., Xiao, J., Yang, Z., Liao, X., Chen, X., Wang, L., & Qin, H. (2023). Hypothalamic supramammillary neurons that project to the medial septum modulate wakefulness in mice. *Communications Biology*, *6*(1). https://doi.org/10.1038/s42003-023-05637-w

Liu, X., Ramirez, S., Pang, P. T., Puryear, C. B., Govindarajan, A., Deisseroth, K., & Tonegawa, S. (2012). Optogenetic stimulation of a hippocampal engram activates fear memory recall. *Nature*, *484*(7394), 381–385. https://doi.org/10.1038/nature11028

López-Ferreras, L., Eerola, K., Mishra, D., Shevchouk, O. T., Richard, J. E., Nilsson, F. H., Hayes, M. R., & Skibicka, K. P. (2019). GLP-1 modulates the supramammillary nucleus-lateral hypothalamic neurocircuit to control ingestive and motivated behavior in a sex divergent manner. *Molecular Metabolism*, *20*, 178–193. https://doi.org/10.1016/j.molmet.2018.11.005

López-Ferreras, L., Eerola, K., Shevchouk, O. T., Richard, J. E., Nilsson, F. H., Jansson, L. E., Hayes, M. R., & Skibicka, K. P. (2020). The supramammillary nucleus controls anxiety-like behavior; key role of GLP-1R. *Psychoneuroendocrinology*, *119*. https://doi.org/10.1016/j.psyneuen.2020.104720

Marcus, D. J., Bedse, G., Gaulden, A. D., Ryan, J. D., Kondev, V., Winters, N. D., Rosas-Vidal, L. E., Altemus, M., Mackie, K., Lee, F. S., Delpire, E., & Patel, S. (2020). Endocannabinoid Signaling Collapse Mediates Stress-Induced Amygdalo-Cortical Strengthening. *Neuron*, *105*(6), 1062-1076.e6. https://doi.org/10.1016/j.neuron.2019.12.024

Mueller, N. K., Dolgas, C. M., & Herman, J. P. (2004). Stressor-selective role of the ventral subiculum in regulation of neuroendocrine stress responses. *Endocrinology*, *145*(8), 3763–3768. https://doi.org/10.1210/en.2004-0097

Nettle, D., & Bateson, M. (2012). The evolutionary origins of mood and its disorders. In *Current Biology* (Vol. 22, Issue 17). https://doi.org/10.1016/j.cub.2012.06.020

Pan, W. X., & McNaughton, N. (2002). The role of the medial supramammillary nucleus in the control of hippocampal theta activity and behaviour in rats. *European Journal of Neuroscience*, *16*(9), 1797–1809. https://doi.org/10.1046/j.1460-9568.2002.02267.x

Pedersen, N. P., Ferrari, L., Venner, A., Wang, J. L., Abbott, S. B. G., Vujovic, N., Arrigoni, E., Saper, C. B., & Fuller, P. M. (2017). Supramammillary glutamate neurons are a key node of the arousal system. *Nature Communications*, *8*(1). https://doi.org/10.1038/s41467-017-01004-6

Peng, B., Xu, Q., Liu, J., Guo, S., Borgland, S. L., & Liu, S. (2021). Corticosterone attenuates reward-seeking behavior and increases anxiety via D2 receptor signaling in ventral tegmental area dopamine neurons. *Journal of Neuroscience*, *41*(7), 1566–1581. https://doi.org/10.1523/JNEUROSCI.2533-20.2020

Qin, H., Fu, L., Jian, T., Jin, W., Liang, M., Li, J., Chen, Q., Yang, X., Du, H., Liao, X., Zhang,

K., Wang, R., Liang, S., Yao, J., Hu, B., Ren, S., Zhang, C., Wang, Y., Hu, Z., … Chen, X. (2022). REM sleep-active hypothalamic neurons may contribute to hippocampal social-memory consolidation. *Neuron*, 1–15. https://doi.org/10.1016/j.neuron.2022.09.004

Ryan, T. J., Roy, D. S., Pignatelli, M., Arons, A., & Tonegawa, S. (2015). Engram Cells Retain Memory Under Retrograde Amnesia. *Science*, *348*(6238), 1007–1013. https://doi.org/10.1126/science.aaa5542

Shi, H. J., Wang, S., Wang, X. P., Zhang, R. X., & Zhu, L. J. (2023). Hippocampus: Molecular, Cellular, and Circuit Features in Anxiety. *Neuroscience Bulletin*, *39*(6), 1009–1026. https://doi.org/10.1007/s12264-023-01020-1

Strange, B. A., Witter, M. P., Lein, E. S., & Moser, E. I. (2014). Functional organization of the hippocampal longitudinal axis. In *Nature Reviews Neuroscience* (Vol. 15, Issue 10, pp. 655–669). Nature Publishing Group. https://doi.org/10.1038/nrn3785

Sun, H., Li, Z., Qiu, Z., Shen, Y., Guo, Q., Hu, S. W., Ding, H. L., An, S., & Cao, J. L. (2023). A common neuronal ensemble in nucleus accumbens regulates pain-like behaviour and sleep. *Nature Communications*, *14*(1). https://doi.org/10.1038/s41467-023-40450-3

Sun, X., Bernstein, M. J., Meng, M., Rao, S., Sørensen, A. T., Yao, L., Zhang, X., Anikeeva, P. O., & Lin, Y. (2020). Functionally Distinct Neuronal Ensembles within the Memory Engram. *Cell*, *181*(2), 410-423.e17. https://doi.org/10.1016/j.cell.2020.02.055

Tang, H., Wu, G. S., Xie, J., He, X., Deng, K., Wang, H., Xu, F., & Luo, H. R. (2016). Brain-wide map of projections from mice ventral subiculum. *Neuroscience Letters*, *629*, 171–179. https://doi.org/10.1016/j.neulet.2016.07.014

Tonegawa, S., Liu, X., Ramirez, S., & Redondo, R. (2015). Memory Engram Cells Have Come of Age. *Neuron*, *87*(5), 918–931. https://doi.org/10.1016/j.neuron.2015.08.002

Tonegawa, S., Morrissey, M. D., & Kitamura, T. (2018). The role of engram cells in the systems consolidation of memory. *Nature Reviews Neuroscience*, *19*(8), 485–498. https://doi.org/10.1038/s41583-018-0031-2

Yan, J. J., Ding, X. J., He, T., Chen, A. X., Zhang, W., Yu, Z. X., Cheng, X. Y., Wei, C. Y., Hu, Q. D., Liu, X. Y., Zhang, Y. L., He, M., Xie, Z. Y., Zha, X., Xu, C., Cao, P., Li, H., & Xu, X. H. (2022). A circuit from the ventral subiculum to anterior hypothalamic nucleus GABAergic neurons essential for anxiety-like behavioral avoidance. *Nature Communications*, *13*(1). https://doi.org/10.1038/s41467-022-35211-7

Zhang, J., Zhang, J., Yuan, R., Han, W., Chang, Y., Kong, L., Wei, C., Zheng, Q., Zhu, X., Liu, Z., Ren, W., & Han, J. (2024). Inhibition of cannabinoid degradation enhances

hippocampal contextual fear memory and exhibits anxiolytic effects. *IScience*, *27*(2), 108919. https://doi.org/10.1016/j.isci.2024.108919

Zhang, T. R., Larosa, A., Di Raddo, M. E., Wong, V., Wong, A. S., & Wong, T. P. (2019). Negative memory engrams in the hippocampus enhance the susceptibility to chronic social defeat stress. *Journal of Neuroscience*, *39*(38), 7576–7590. https://doi.org/10.1523/JNEUROSCI.1958-18.2019

Zheng, Z., Liu, Y., Mu, R., Guo, X., Feng, Y., Guo, C., Yang, L., Qiu, W., Zhang, Q., Yang, W., Dong, Z., Qiu, S., Dong, Y., & Cui, Y. (2024). A small population of stress-responsive neurons in the hypothalamus-habenula circuit mediates development of depression-like behavior in mice. *Neuron*. https://doi.org/10.1016/j.neuron.2024.09.012